

wheel, rail, two-point contact, normal forces

**Alexandr GOLUBENKO, Alexandr KOSTYUKEVICH**  
**Илья TSYGANOVSKIY\*, Vladimir NOZHENKO**  
East-Ukrainian National University named after V. Dal  
Molodyozhny block, 20a, Lugansk, 91034, Ukraine  
*\*Corresponding author. E-mail: ilyats@list.ru*

## TWO-POINT WHEEL - RAIL CONTACT INVESTIGATION

**Summary.** This paper describes a wheel - rail contact for a case when one contact point is located on the wheel tread while the other is on the wheel flange. The locations of these points are determined for both wheels for given lateral displacement and yaw angle of a wheelset. Numerical simulation results are presented for new and worn rail-wheel profiles in order to demonstrate a developed algorithm.

## ИССЛЕДОВАНИЕ ДВУХТОЧЕЧНОГО КОНТАКТА КОЛЕСА С РЕЛЬСОМ

**Аннотация.** Рассмотрен контакт колеса с рельсом для случая, когда одна точка контакта находится на ободе колеса, а другая на гребне. Положение этих точек определяется для обоих колес колесной пары в зависимости от заданного бокового отбоя и угла виляния. Для демонстрации разработанного алгоритма приведены результаты численного моделирования двухточечного контакта для новых и изношенных профилей колеса и рельса

### 1. INTRODUCTION

There are a lot of works dedicated to wheel – rail contact simulation. Until recently, there was no unique methodology for contact models comparison and validation. The Kalker's CONTACT [1] program was often used for benchmark. In Knothe's review of the history of wheel – rail contact mechanics he states, "Nowadays, most problems of rolling contact mechanics can be solved using Kalker's programs". But CONTACT program uses so – called «exact» rolling contact theory, and this fact makes it very slow and therefore useless for railway vehicle simulation. That's why today the most models used for railway vehicle simulation introduce a number of simplifications.

Having the aim to compare accuracy and efficiency of existing theoretical models of wheel – rail contact and those that will be developed, a group of researchers of Manchester Metropolitan University have proposed contact benchmark. The aims of the test are: contact path size, shape and position detection; normal pressure distribution; tangent pressure distribution. Two different cases are considered: A) Prescribed single wheel or wheelset contact study, B) Dynamic vehicle simulation. Case A is split into two subcases: Case A-1 – Normal contact, Case A-2 – Tangential contact. The input parameters for Case A-1, which will be considered in this article, are: Wheel profiles, Rail profiles, Wheel rolling radius, Gauge width, Flange-back spacing, Vertical load. The variables are Lateral displacement and Yaw angle. The benchmark results for the most popular commercial multibody software are presented in [3].

Nearly the same time with Manchester Benchmark FRA/DTT Cooperation Team из John A. Volpe National Transportation Systems Center proposed Dynamic Wheel/Rail Benchmark Single Wheelset without Friction [4]. This very simple Benchmark is intended to analyze normal contact force calculations and modeling of flanging with impacts. But the authors state that it is expected to find different results due to differences in coding assumptions. The main difference from Case A-1 of Manchester Benchmark despite their similarity is that it is intended to examine the dynamical behavior of the wheelset, and in the former a static wheelset is considered.

But whether the static wheelset or its dynamic behavior are examined, the exact algorithm is necessary for initial contact points detection. The ability of two – point contact detection is in special demand for this algorithm. All existing algorithms of initial contact points detection can be separated into two groups. The first group treats wheel and rail bodies as rigid ones and contact points detection task is solved as pure geometrical [5-7]. The second group consider contacting bodies as elastic and the contact points detection task is solved using geometrical methods and elasticity theory methods [8,9,10].

Let's take a look at the most popular methods from the first group. In «Universal mechanism» software [5] the contact points are detected separately for left and right wheel – rail contact pairs. It is assumed that the wheel profile has two degrees of freedom relatively to rail: yaw angle and lateral shift. The 2D task is solved. At the first step for every point on rail profile the corresponding point on wheel is found and the distances between them are calculated. Then after the consecutive bypassing all the points the ones having the minimal distance between are detected. It is assumed that when the lateral shift gets its critical value the two point contact takes place, and from this time the contact points positions in the corresponding coordinate frames stay constant and the wheel will shift together with rail in lateral direction. In future, the wheel can return to single point contact, or when the normal reaction from the rail is zero, proceed to the roll in regime.

The methods [6] and [7] has the same problem description. The two arbitrary surfaces of the wheel and rail are considered. It is assumed that the wheelset is “hang up” over the rails and has two degrees of freedom: lateral shift and yaw angle. The contact points detection is performed simultaneously for both left and right wheel – rail contact pairs. In work [6] the iterative procedure of contact points detection is based on wheelset pitch angle modification until the minimum distance between left wheel and rail surfaces is not equal to the minimum distance between right wheel and rail surfaces. In work [7] the distance difference is treated as pitch angle function and the minima of this function is detected with the use half division method. For both solutions specified the two point contact detection is quite difficult as the task of search of minimum value for function which has multiple minima has to be solved.

In the methods of the second group the penetration is allowed and is used for resulting contact forces detection. This formulation of contact points detection problem is more suitable for two – point contact identification. In the paper [9] the concept of «difference surfaces» is introduced, which are defined as the difference between wheel and rail surfaces. If such difference surface presents only positive values, then the rail and the wheel are not in contact. If the difference surface shows at least some negative values, then there are one or more contact areas. In paper [10] the concept of «intersection volume» is introduced, which is formed by rail and wheel surfaces points by the given conditions. The fictitious contact spring is inserted between wheel and rail and its stiffness is updated during the solution process. Then using the one of methods presented, the maximal indentation between wheel and rail is calculated and after solution of the linear vector equations system the contact forces are calculated and then the new wheelset position is detected. We will use this model as basis for our research.

## 2. WHEEL – RAIL CONTACT MODEL

Let's introduce the moving and fixed coordinate frames (see Fig. 1) For a fixed coordinate frame OXYZ the origin is located in the middle of the gauge on the rail heads level, x axis is directed along the rail, y axis – across the rail and z axis points upwards. The origin of a moving coordinate frame

GXYZ is located in the mass center of the wheelset, Y axis is directed along the axle of the wheelset and Z axis points upwards. The absolute coordinates of GXYZ will be denoted as  $x_g, y_g, z_g$ , and  $\theta_x, \theta_y, \theta_z$  will denote angles between x and X, y and Y, z and Z respectively.

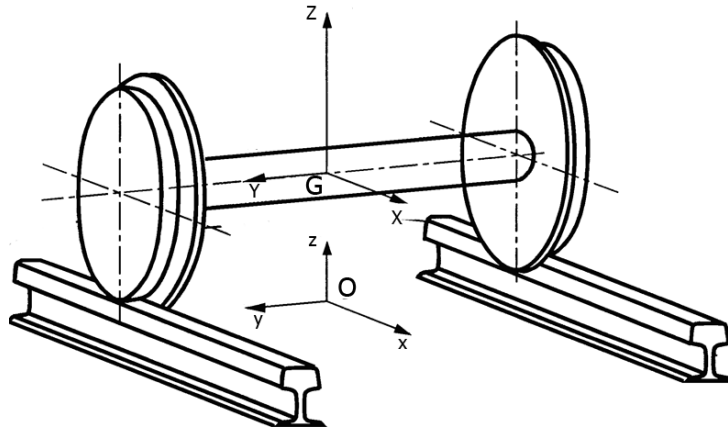


Fig. 1. Moving and fixed coordinate frames

Рис. 1. Подвижная и неподвижная системы координат

In the general case the unconstrained wheelset has six degrees of freedom. If the contact is treated as continuous, then this number reduces to two- lateral shift  $y_g$  and yaw angle  $\theta_z$ , which will be treated as independent variables. For the rest four dependent variables determination we will add four fictitious spring elements for each dependent variable. For a static wheel set all forces and moments generated by these elements and contact forces must satisfy the following vector equilibrium equations:

$$\begin{aligned} \sum_{i=1,3} k_{el}^i (x_i - l_{0i}) \bar{N}_i + \sum_{h=1}^{n_{CS}} F_{cs}^h + \sum_{g=1}^{n_{CD}} F_{cd}^g &= 0 \\ \sum_{i=1,3} k_{rot}^i \theta_i \bar{N}_i + \sum_{h=1}^{n_{CS}} (\bar{G}P_s^h \times F_{cs}^h) + \sum_{g=1}^{n_{CD}} \bar{G}P_d^g \times F_{cd}^g &= 0 \end{aligned} \quad (1)$$

where:

$i$  – the index vary from 1 to 3 denotes x, y, z components of OXYZ coordinate frame,

$k_{el}^i$  – the stiffness of the spring acting along the  $i^{\text{th}}$  axis of GXYZ,

$k_{rot}^i$  – the stiffness of the torsional spring, which counteracts rotation around the  $i^{\text{th}}$  axis of GXYZ,

$l_0$  – the length of the undeformed spring,

$n_{CS}, n_{CD}$  – number of contact points on the left and right wheels respectively,

$\bar{F}_{cs}^h$  – contact forces at the  $h^{\text{th}}$  contact point on the left wheel,

$\bar{F}_{cd}^g$  – contact forces at the  $g^{\text{th}}$  contact point on the right wheel,

$\bar{G}P_s^h$  – vector(s), directed from  $G$  to  $h^{\text{th}}$  contact points on the left wheel,

$\bar{G}P_d^g$  – vector(s), directed from  $G$  to  $g^{\text{th}}$  contact points on the right wheel,

$\bar{N}_i$  – unit vector, directed along the  $i^{\text{th}}$  axis of OXYZ.

## 2.1. Intersection volume and maximum indentation determination

In the original work [10] the conception of «intersection volume» is introduced. This is a volume, produced by wheel and rail surfaces intersection, as is shown on Fig. 2. The rail surface is generated

by extrusion of its 2D profile along the  $x$  axis of  $Oxyz$  coordinate frame, and the wheel surface is generated by revolution of its 2D profile around  $Y$  axis of  $GXYZ$  coordinate frame. The criterion of including points in the intersection volume is defined with the use of calculation and analyzing the scalar product of vectors joining the wheel and rail points and normals to these points. This approach matches significant computational difficulties if used as subprogram for Manchester Benchmark. The UIC60 rail and S1002 wheel profiles, which are used for input in Manchester Benchmark, are rather high discretized and contains 495 and 400 points respectively. Thus the generated surfaces can contain the hundreds thousands nodes. This fact significantly increase the required memory limit, and bypassing and analyzing of all points become unaffordably time consuming.



Fig. 2. Intersecting area  
Рис. 2. Зона пересечения

Therefore much faster algorithm for intersection volume construction is required. As the rail is assumed to be straight, there is no need for rail surface generation for determination of the points to get “inside” the rail, the memory storage of its profile in  $x=0$  plane is strong enough. Then for an examination whether the point is in intersection volume, the 2D task is solved, where the  $x$  coordinate of rail profile is set to the  $x$  coordinate of the current point. As the profile is given as polyline, then its internal part can be represented as the sequence of trapezoids with a prescribed length of the baselines that are parallel to the  $z$  axis of the  $Oxyz$  coordinate frame, and one side joining the neighboring points of rail profile (Fig. 3a). The fact of location the point inside the trapezoid is established with the analyze of skew product of vectors joining this points with the trapezoid’s vertexes (Fig. 3b). The  $p(x, y)$  and  $q(u, v)$  vectors skew product is defined with the following formula:

$$[p, q] = xv - yu \quad (2)$$

If all skew products have the same sign, then the points lays inside the trapezoid and outside otherwise. If the point lays inside, the we add it to the intersection volume and the corresponding point on the rail is determined by the normal and rail intersection.

For a maximal indentation determination we will use the maximum distance method introduced in [10]. For every point for intersection volume, corresponding to rail, we will find point on the wheel, which is located at the maximum distance. Let’s denote vector, which joins point  $P_W$  on the wheel with point  $P_R$  on the rail, by  $\bar{V}_{WR}$ . Then the maximal indentation  $I_{\max}$  will be defined as maximum from the  $\bar{V}_{WR}$  vector’s projections on point  $P_W$  normal:

$$I_{\max} = \max((\bar{V}_{WR}, \bar{N}_{P_W})) \quad (3)$$

And the points with maximum indentation will be contact points.

## 2.2. Two – point contact

Since the intersection volume is created, it is necessary to find the number of contact points. The condition is required, which will split the produced set of points into the subsets, when the intersection

volume consists of two non-intersecting sets of points. It should be taken into account, that the rail profile used in our study, is defined as the ordered collection of points. On Fig. 5 two wheel surface fragments are shown, produced from this profile. The marked points are the points which are included in the intersection volume. On Fig. 5b we can see, that there is a “jump” between the points included to the intersection volume. Therefore for the intersection volume splitting we will use the following rule: if there is a «jump» between indexes of the points included to the intersection volume, then the volume should be split into the two non- intersecting volumes and search for maximum indentation should be performed in each of them.

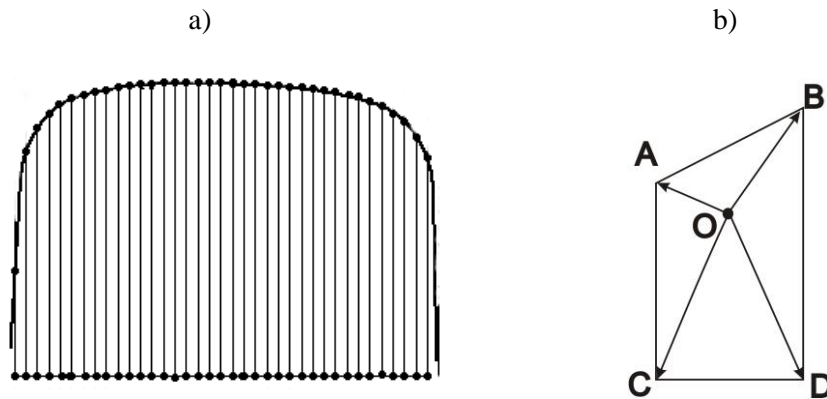


Fig. 3. a) Trapezoids inside the rail profile; b) A scheme for the point inside the trapezoid determination  
Рис. 3. а) Трапеции в профиле рельса; б) Схема для определения попадания точки в трапецию

The flowchart of the used algorithm is shown on Fig. 4

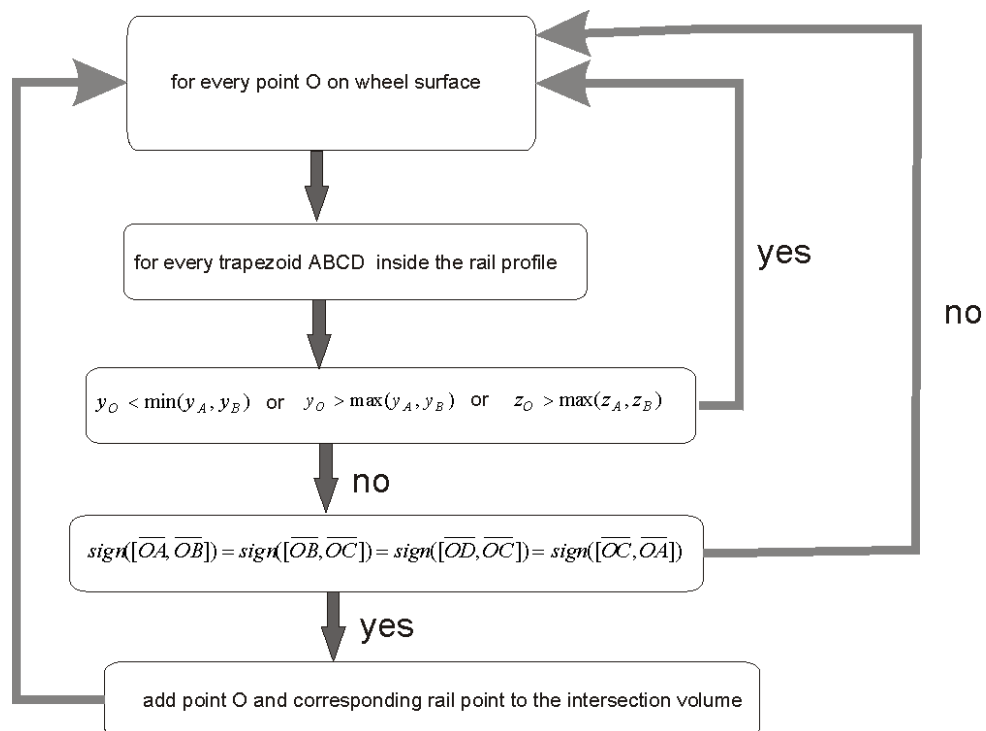


Fig. 4. The flowchart of the intersection volume filling algorithm  
Рис. 4. Блок – схема алгоритма построения объема пересечения

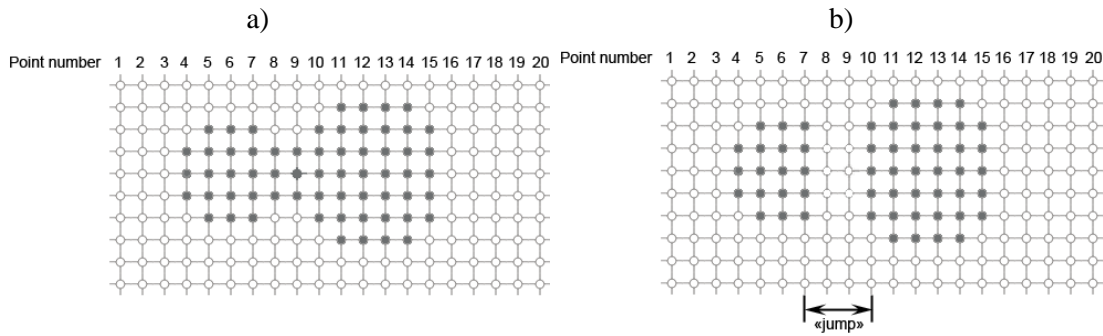


Fig. 5. a) Point on the surface with no “jump”; b) Point on the surface with “jump”

Рис. 5. а) Точки на поверхности колеса без «скачка»; б) Точки на поверхности колеса со скачком

### 2.3. Elastic contact model and normal contact forces calculation

The normal reactions in the detected initial contact points for left and right rail are defined with formulas:

$$\begin{aligned} F_{CL} &= -I_{\max}^L k_c N_{LW} \\ F_{CR} &= -I_{\max}^R k_c N_{RW} \end{aligned} \quad (4)$$

where:

$I_{\max}^L, I_{\max}^R$  – maximal indentation for left and right rail respectively,

$N_{LW}, N_{RW}$  – unit vectors in contact points for a left and right wheel respectively,

$k_c$  – stiffness of fictitious contact spring inserted between wheel and rail (Fig. 6).

The  $k_c$  value is determined during the iteration process. For  $x_g, y_g, z_g, \theta_x, \theta_y, \theta_z$  variables the vector equations system (1) is solved. As a criterion for the exit from the iteration process the following condition is used:

$$\begin{aligned} \sum F_{CL} &\leq -F_L \\ \sum F_{CR} &\leq -F_R \end{aligned} \quad (5)$$

where:  $F_L$  and  $F_R$  – are prescribed loading vectors for left and right wheel respectively.

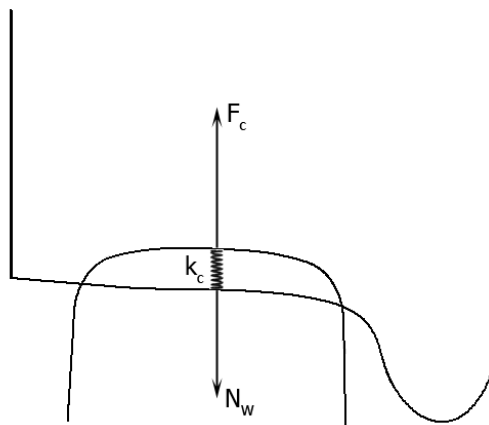


Fig. 6. Fictitious contact spring between wheel and rail.  $k_c$  -spring stiffness,  $N_w$  – normal to wheel surface,  $F_c$  – normal reaction from rail

Рис. 6. Фиктивная пружина между колесом и рельсом.  $k_c$  – жесткость пружины,  $N_w$  – нормаль к поверхности колеса,  $F_c$  – нормальная реакция со стороны рельса

The flowchart of the used algorithm is shown on Fig. 7

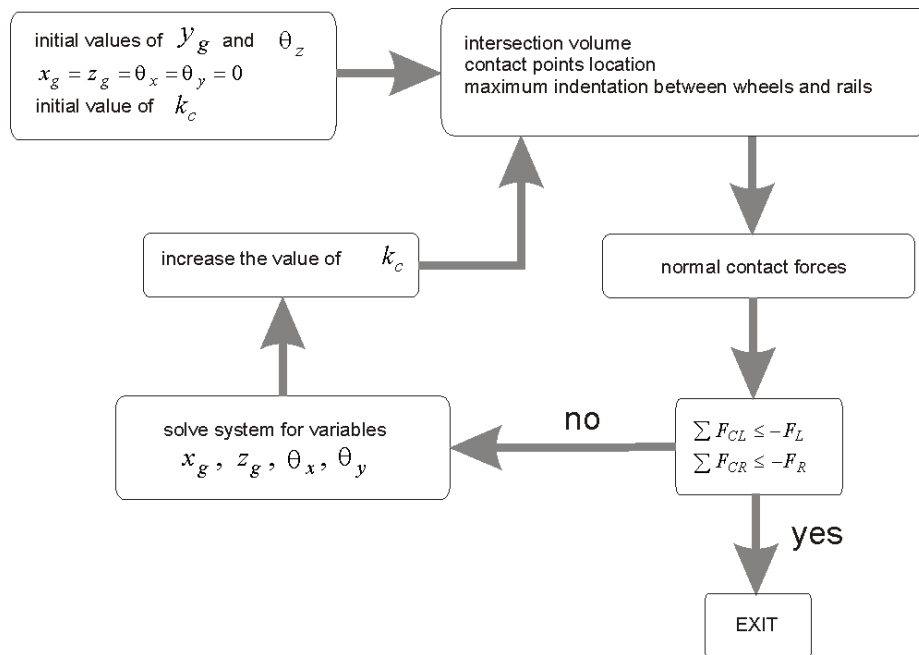


Fig. 7. The flowchart of initial contact points detection algorithm

Рис. 7. Блок схема алгоритма поиска точек начального касания

### 3. NUMERICAL RESULTS

Having the aim to test the performance of the developed algorithm, a software was developed using C++ Builder 6.0 program environment. The new and worn profiles were examined, that are used as inputs for Manchester Benchmark. Those profiles with detected point of initial contact are shown on Fig. 8. The digits over the wheel profile denote lateral shift of the wheelset. The thin lines connect detected contact pairs for one – point contact, the thick lines connect bicontact points.

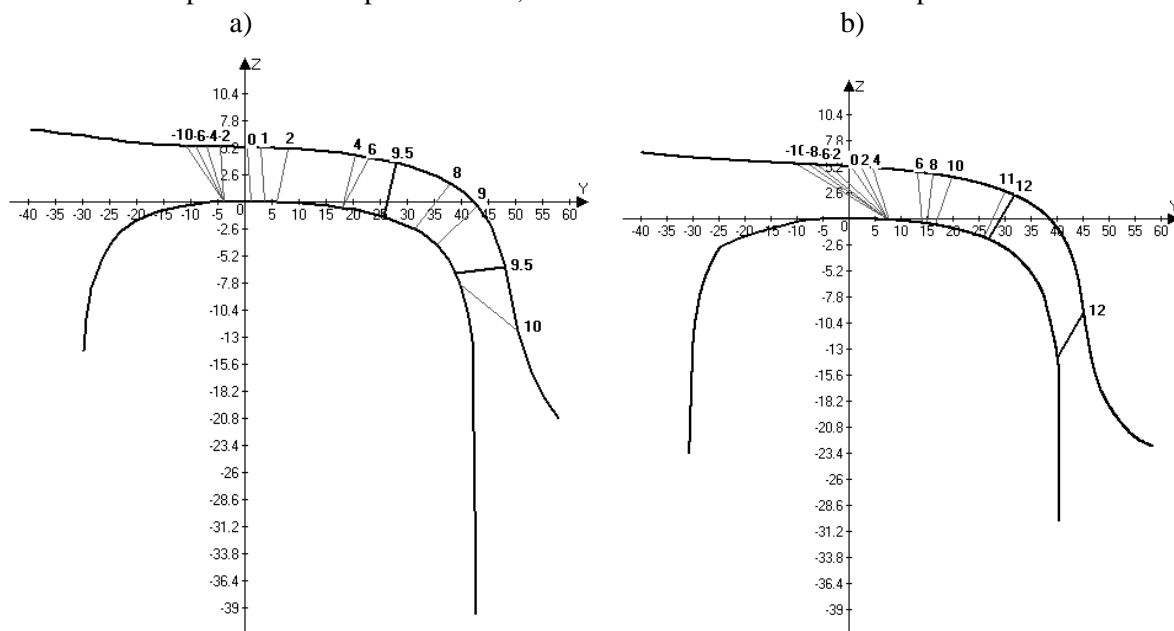


Fig. 8. a) contact pairs for new wheel and rail profiles; b) contact pairs for worn wheel and rail profiles

Рис. 8. а) контактные пары точек для новых профилей колеса и рельса; б) контактные пары точек для изношенных профилей колеса и рельса

#### 4. CONCLUSIONS

The faster version of initial contact points detection algorithm presented in [10] was developed. The numerical results showed the difference near the 200% in computation speed. The results of algorithm performance are presented. It can be seen, that difference between value of lateral shift for new and worn wheel and rail profiles when flanging starts is approximately 2mm.

#### References

1. Kalker J.: *Three-Dimensional Elastic Bodies in Rolling Contact*. Kluwer Academic Publishers, Norwell, 1990.
2. Knothe K.: *History of wheel/rail contact mechanics: from Redtenbacher to Kalker*. *Vehicle System Dynamics*, vol. 46(1), 2008, pp. 9-26.
3. Shackleton P., Iwnicki S.D.: *Comparison of wheel-rail contact codes for railway vehicle simulation: an introduction to the Manchester Contact Benchmark and initial results*. *Vehicle System Dynamics*, vol. 46(1), 2008, p. 129-149.
4. *Call for Simulations: Dynamic Wheel/Rail Benchmark Single Wheelset without Friction*. US DOT Volpe Center, 2005.
5. *Моделирование динамики железнодорожных экипажей*. Руководство пользователя ПО Универсальный механизм 6.0, 2010, с. 48-57. [http://www.umlab.ru/download\\_rus.htm](http://www.umlab.ru/download_rus.htm)
6. Zili Li: *Wheel-Rail Rolling Contact & Its Application to Wear Simulation*. Delft University Press, Amsterdam, 2002, pp. 67-76.
7. Костюкевич А.И.: *Численная и экспериментальная идентификация процесса сцепления колес локомотива с рельсами*. дисс. к.т.н. Луганск, 1991, с. 230.
8. Shabana A.A., Zaaza K.E., Escalona J.L., Sany J.R.: *Development of elastic force model for wheel-rail contact problems*. *Journal of Sound and Vibration*, vol. 269, 2004, pp. 295-325.
9. Meli E., Auciello J., Malvezzi M., Papini S., Pugi L., Rindi A.: *Determination of wheel rail contact points with semi analytic methods*. *Multibody System Dynamics*, Vol. 20, 2008, pp. 327-358.
10. Bozzone M., Pennestri E., Salvini P.: *A compliance based method for wheel-rail contact analysis*. 8<sup>th</sup> International Conference on Contact Mechanics and Wear of Rail/Wheel Systems, Florence, 2009.

Received 28.05.2010; accepted in revised form 04.06.2011